Chapter 8

Omnidirectional Circularly Polarized Antenna with High Gain in Wide Bandwidth

Bin Zhou, Junping Geng, Xianling Liang, Ronghong Jin and Guanshen Chenhu

Additional information is available at the end of the chapter

http://dx.doi.org/10.5772/66011

Abstract

A novel omnidirectional circularly polarized (CP) slot array antenna with high gain is proposed, which is based on the coaxial cylinder structure, and the orthogonal slots radiated the circular polarization wave around the cylinder. Further, the improved dual circularly polarized (CP) omnidirectional antenna based on slot array in coaxial cylinder structure is presented too, and two ports are assigned in its two side as left hand circularly polarized (LHCP) port and right hand circularly polarized (RHCP) port, respectively. The simulation and experiment results show their novelty and good performance of omnidirectional circular polarization with about 5 dBi gain in 5.2–5.9 GHz.

Keywords: omnidirectional circularly polarized (CP) antenna, slot array

1. Introduction

Omnidirectional circularly polarized (CP) antenna is a very good choice for wireless transmission and fast networking in wireless communication, which provides omnidirectional coverage, and is insensitive to the orientations of the waves. In addition, the circularly polarization will suppress the multipath interference in the complex environment [1].

In recent years, many kinds of omnidirectional CP antennas are investigated for the development of communication technology. In references [2–4], some planar microstrip omnidirectional CP antennas with dual-band are proposed, which are small, but the work bands are narrow. In references [5, 6], the omnidirectional CP dielectric resonator antennas (DRAs) are proposed, whose size is very small for the high permittivity, and their available impedance bandwidth can reach to 20% while the CP bandwidth is only 3–8% for the 3-dB axial-ratio

(AR). In reference [7], a CP antenna is designed which combines monopole and loop radiators to realize omnidirectional CP property, and the impedance bandwidth is about 15%. In reference [8], a compact size omnidirectional CP antenna is studied, in which four bended monopoles are simultaneously excited by feeding network. A broadband omnidirectional CP antenna is proposed in [9], of which the impedance bandwidth reaches to 45%, but its gain is not stable and high in the available bandwidth.

In another side, for a RF receiver which needs to receive electromagnetic signals with any polarizations mode and from any directions on the ground, the dual CP omnidirectional antenna is also very significant and valuable. The dual CP omnidirectional antenna is widely used, such as in wireless communications, radio broadcasting, and navigation radar [1, 11, 12]. In recent years, there are many researches about omnidirectional antenna and CP antenna. In reference [3], a miniaturization of omnidirectional CP antenna relies on folding the antennas patch underneath itself, decreasing overall footprint, which is small, but with a narrow bandwidth of only 0.6% (2.392–2.407 GHz) and the axial ratio in some directions of the omnidirectional plane is higher than 3 dB. For the antenna proposed in reference [13], by introducing several inclined slits to the diagonal and sidewalls of the rectangular dielectric resonator (RDR) and also deducting a rectangular part of the top wall of the linearly polarized (LP) rectangular dielectric resonator antenna (RDRA), degeneracy modes are excited to generate the circularly polarized (CP) fields, while the bandwidth is narrow and the gain fluctuation in the omnidirectional plane is higher than 5 dB from the results of the radiation patterns, so it does not perform well in the omnidirectional character. Literature [14] reports a dual CP antenna which is excited at the second-order mode to generate the conical radiation pattern and is fed by a hybrid coupler to obtain the dual CP operation, but it realizes a conical beam instead of an omnidirectional coverage radiation pattern. There are only a few researches about omnidirectional dual CP antenna. In literature [15], an omnidirectional dual-band dual circularly polarized microstrip antenna is proposed, while the dual circularly polarization means that the antenna provides different single RHCP and LHCP in its two different bandwidths, respectively, so it is single circularly polarized antenna in the specific frequency bandwidth actually. In reference [16], a dual-CP omnidirectional antenna is proposed, which consists of four tilted dipoles with parasitic elements for each sense of circular polarization.

To achieve compact omnidirectional CP antenna and to overcome the shortcomings of previous antenna listed above, here we design two kinds of omnidirectional circularly polarized slot array antenna, one is single CP polarized antenna, and the other one is the dual CP omnidirectional antenna. So in this chapter, the antenna design includes two parts:

1. An omnidirectional circularly polarized slot array antenna with high gain in a wide bandwidth.

2. Dual circularly polarized omnidirectional antenna with slot array on coaxial cylinder.

In the first part of this chapter, we propose our idea of omnidirectional circularly polarized slot array antenna, continually, introduce the design principle of this CP antenna, and the method to design the omnidirectional CP antenna. Later, an example is given, and the experimental results show its novelty and good performance.

http://dx.doi.org/10.5772/66011

In the second part of this chapter, we introduce the antenna with two ports in its two sides to realize dual circular polarization, and these two ports are assigned in its two side as left hand circularly polarized (LHCP) port and right hand circularly polarized (RHCP) port, respectively. The design principle is much the same with the first antenna presented but much more simple and symmetric. And detailed mathematical derivation is presented to prove the antenna's circular polarization property. Same as the first part of this chapter, results and discussion are presented in the final of the section to show its novel performance.

2. An omnidirectional circularly polarized slot array antenna with high gain in a wide bandwidth

In this section, a novel omnidirectional CP antenna based on the coaxial cylinder waveguide with slots array around the cylindrical conductor shell is designed. The CP wave is radiated by the four orthogonal slots pairs with a wavelength interval around the cylinder shell, and combined the omnidirectional CP wave. Four ring slot pairs along the axis construct a slot array around the cylinder shell that achieves the stable high gain. Furthermore, it is convenient to increase or reduce the number of the basic slot array elements along the axis to adjust the antenna gain for wider application.

2.1. Antenna structure

The structure of the proposed omnidirectional CP antenna is shown in **Figure 1**. It is based on the slots array in the coaxial cylinder, and the interval of the inner and outer conductors is filled by Teflon. The thickness of the outer cylinder conductor is t = 1.5 mm. The antenna includes three parts: radiation slot array, impedance matching part, and feeding part.

The orthogonal slot pairs are the basic radiation elements that are symmetrically distributed around the cylinder conductor shell, as shown in **Figure 1**. These elements will radiate the omnidirectional CP wave. Four of the basic radiation elements group along the axis constructs the slot array.

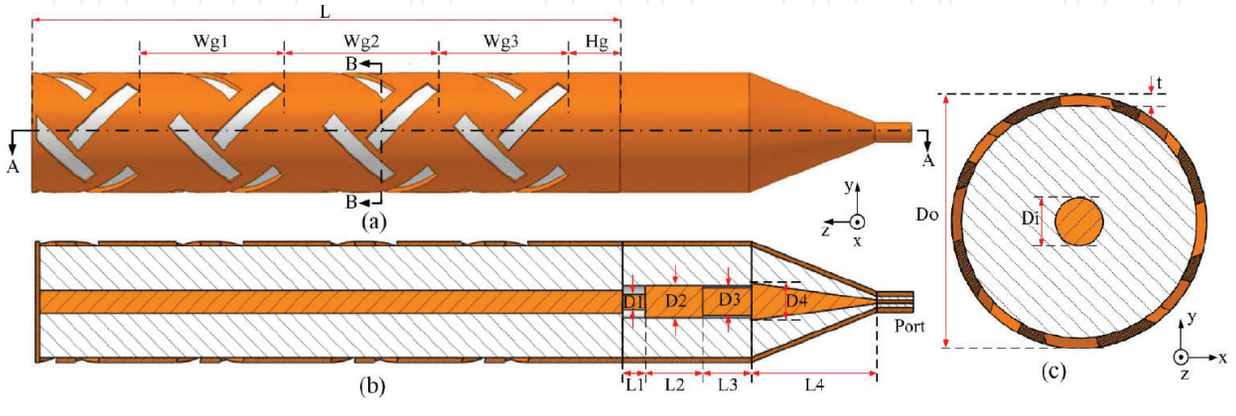

Figure 1. Geometry of the omnidirectional CP antenna. (a) Side view. (b) A-A section view. (c) B-B section view.

In **Figure 1(b)**, three coaxial cylinders L1, L2, and L3 form the impedance matching part. In order to install the small SMA adaptors with a characteristic impedance of 50 Ω to the large-size radiation part with an input impedance varying with the frequency, the coaxial cylinders L1, L2, and L3 with optimized characteristic impedance and electrical length are designed based on the theory of transmission line.

The feeding part L4 is a coaxial tapered line with stable characteristic impedance by keeping a constant ratio of outer and inner radius, which will connect the small-size SMA adaptor to the large-size matching part.

2.2. Design principle

The geometry structure of the slot pairs are shown in **Figure 2**. One slot tilts at 45°, while the other tilts at -45°. Moreover, they are placed with interval $\lambda_g/4$ (λ_g is the medium wavelength) distance along the axis, and the waves radiated from the slot pairs are orthogonal to each other with 90° phase difference, so that they achieve the RHCP property [10]. In another side, the slot is equivalent to a magnetic current source like a dipole tilted at an angle of 45°, the slot is designed with length $L_s = 2\lambda_g/2$.

Four of the slot pairs uniformly distributed around the cylinder conductor shell can be regarded as the basic omnidirectional CP element which is shown in **Figure 1(c)**. For high-gain, four rounds of the basic elements along the axis construct the slot array in **Figure 1(b)**.

The four rounds of elements are placed at an interval distance $W_g = \lambda_g$, so that the waves radiated from every element of the slot array keep the same phases. The filled substrate is Teflon with permittivity $\varepsilon_r = 2.1$, so the interval between the slot array elements is $\lambda_g = 0.7$

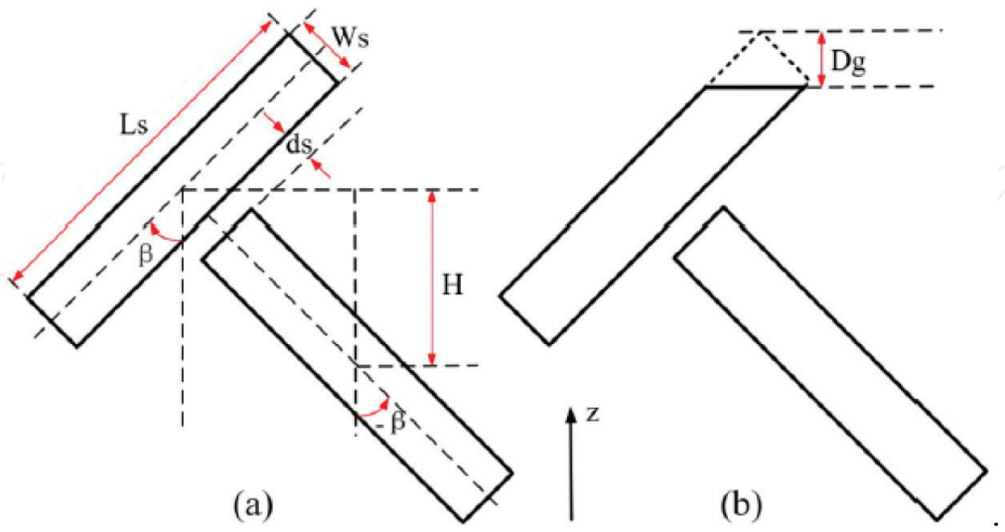

Figure 2. Geometry of slot pairs on outer conductor of the coaxial cylinder. (a) Normal slot pairs. (b) Changed slot pairs.

λ_0 (λ_0 is the space wavelength). While the slot element close to the end is unique as shown in **Figure 2(b)**, it is cut at a length as shown in **Figure 2(a)**. The end element is practically like a matched load to radiate electromagnetic wave and relieves the reflected wave in the shortened terminal of the coaxial cylinder, which ensures the traveling wave running in this structure and improves radiation efficiency of the antenna. So, the antenna performs stable high gain in a wide CP and impedance bandwidth.

2.3. Simulate verification

The omnidirectional CP antenna is simulated and optimized using CST Microwave Studio software based on the finite integration technique (FIT). The optimized geometric parameters are summarized in **Table 1**.

D_o	32 mm	D4	10 mm
D_i	6 mm	L1	6.1 mm
L	161.1 mm	L2	15.8 mm
W_g1	39.59 mm	L3	13.2 mm
W_g2	42.27 mm	L4	40 mm
W_g3	35.77 mm	Ls	23.7 mm
Hg	14 mm	Ws	4.5 mm
D1	4.2 mm	H	11.8 mm
D2	8.7 mm	Dg	3.6 mm
D3	7.6 mm	ds	1.65 mm
β	45°		

Table 1. Optimized geometric parameters of the omnidirectional CP antenna.

Figure 3 shows the magnetic field distribution of the antenna at t = 0, T/4, T/2, 3T/4. In order to clearly explain the working principle of the antenna, the magnetic fields on the A-A section and B-B section of the antenna are shown in **Figure 3**. The magnetic fields on the B-B section of the antenna in turn at t = 0, T/4, T/2, 3T/4 display how the omnidirectional CP waves are formed by the basic omnidirectional CP elements in a whole period time (T). The magnetic fields on the A-A section of the antenna detailed shows that the radiated waves always keep the same phase in every slot element. Therefore, the cylindrical slot array antenna performs a stable high gain in the available bandwidth.

At $t = 0$, the magnetic fields are strongest and outward in each slot close to the feeding port, while the fields in the end slot is very weak, as shown in **Figure 3(a)**. At this time, every slot radiates a 45° linear polarized wave. At $t = T/4$, the magnetic fields are the strongest and in outward direction in every slot close to the terminal, while the fields in the slot near the feeding port is very weak as shown in **Figure 3(b)**. At this time, every slot radiates a -45° linear polarized wave. At $t = T/2$ and $t = 3T/4$, the magnetic fields vary in the opposite direction as shown in **Figure 3(c)** and **(d)**, respectively. Thus, there is always a 90° phase difference between the 45° linear polarized wave and the -45° linear polarized wave in all of the slot pairs around the coaxial cylinder.

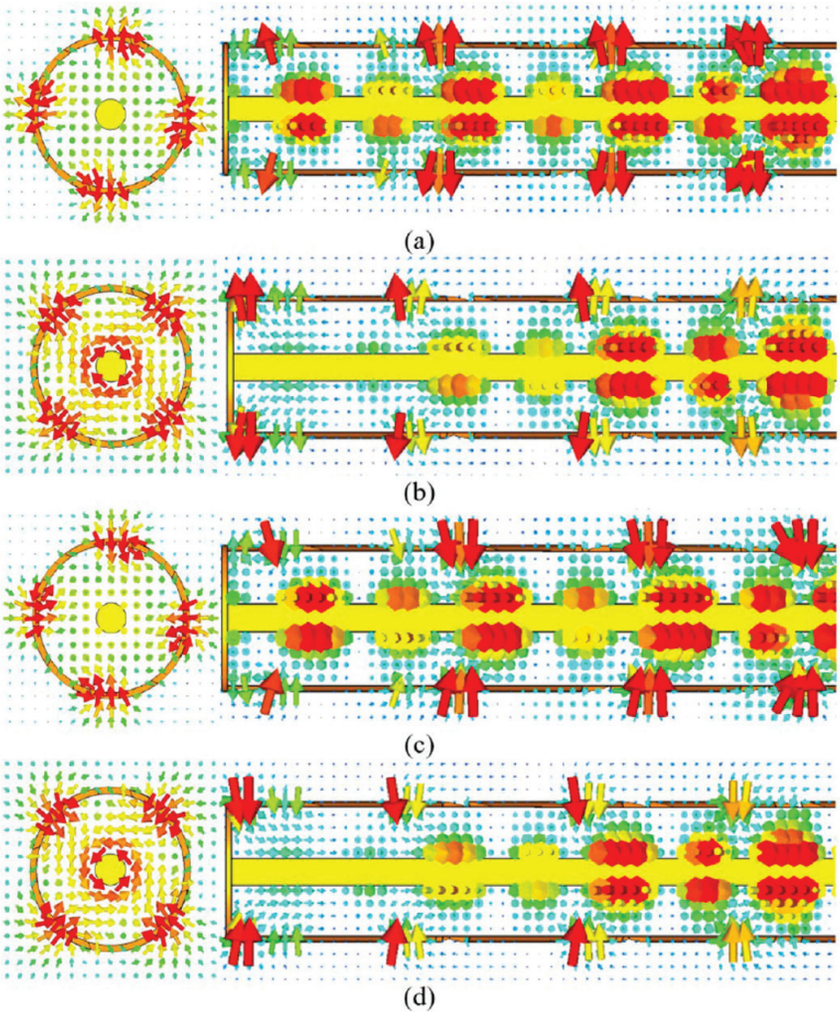

Figure 3. Magnetic fields distribution in (right) A-A section and (left) B-B section of the antenna. (a) $t = 0$. (b) $t = T/4$. (c) $t = T/2$. (d) $t = 3T/4$.

2.4. Results and discussion

Simulated and measured results of the proposed antenna are presented in this section. **Figure 4** shows the test scenario of the omnidirectional CP antenna.

http://dx.doi.org/10.5772/66011

Figure 4. Photograph of the omnidirectional CP antenna being tested in the anechoic chamber.

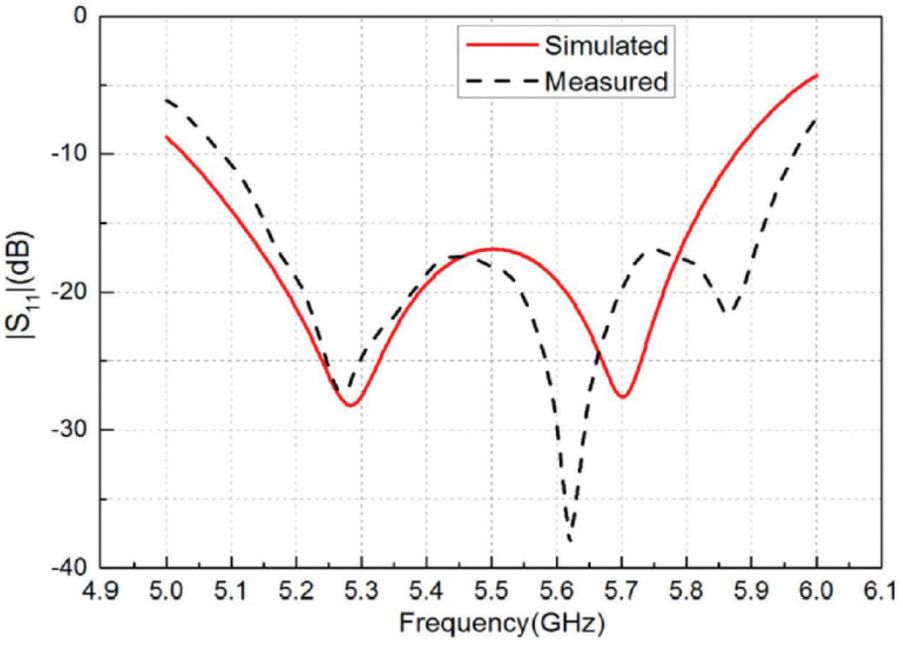

Figure 5. Measured and simulated of the omnidirectional CP antenna.

The simulated and experiment measured return loss are shown in **Figure 5**. It can be observed that the measured impedance bandwidth of $S_{11} < -10$ dB is 16.4% ranging from 5.05 to 5.95 GHz. The measured result shows the same trend with the simulated result, but slightly deflected to the high frequency. It may be because the medium of Teflon is impure, and the real permittivity value of ε_r is smaller than the simulated value of $\varepsilon_r = 2.1$. The simulation and experiment average axial ratio and gain in the horizontal plane (xy-plane) is drawn in **Figure 6**. The experiment measured gain varies from 5 to 7 dBic in 5.1–5.9 GHz, and the average ARs below 3 dB is in 5.1–5.9 GHz. Note that the gains of the experiment are 0.8 dB smaller than simulated near the center frequency, and the average ARs are some worse than the simulated results. Besides the imprecise dialectical constant and the experiment error, the reason for these differences between measured and simulated results is mainly attributed to the manufacturing error because the performance of the antenna is sensitive to the slots size. Generally, the proposed antenna achieves the stable high gain within the available bandwidth. **Figure 7(a)–(c)** shows the simulated RHCP and left-hand CP (LHCP) normalized radiation patterns in the omnidirectional plane (xy-plane), E-plane (yz-plane), and normalized experimental radiation patterns at 5.2, 5.5, and 5.8 GHz, respectively. In **Figure 7**, the cross-polarization in the omnidirectional plane is lower by 16 dB than the copolarization, and the radiation efficiency is 94% in the operating band 5.1–5.9 GHz. The measured and simulated results are very consistent, and the variation in the omnidirectional plane is very small, which means that the proposed antenna has good omnidirectional characteristics.

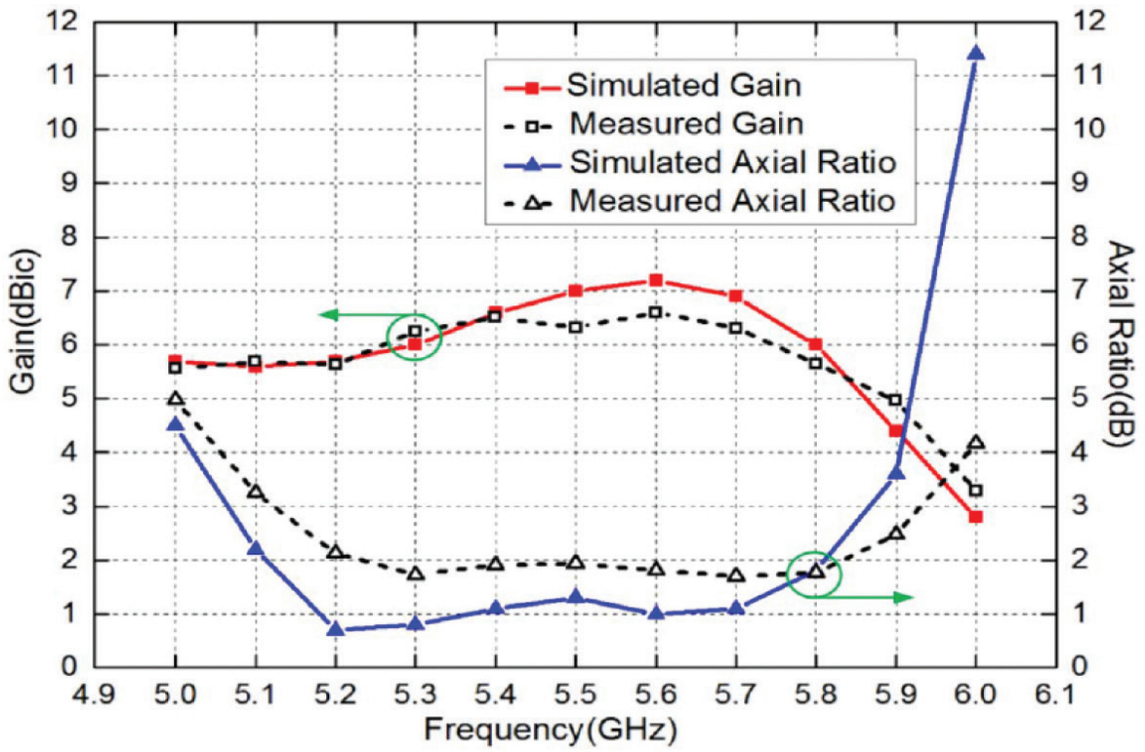

Figure 6. Measured and simulated gain and average axial-ratio results of the omnidirectional CP antenna.

http://dx.doi.org/10.5772/66011

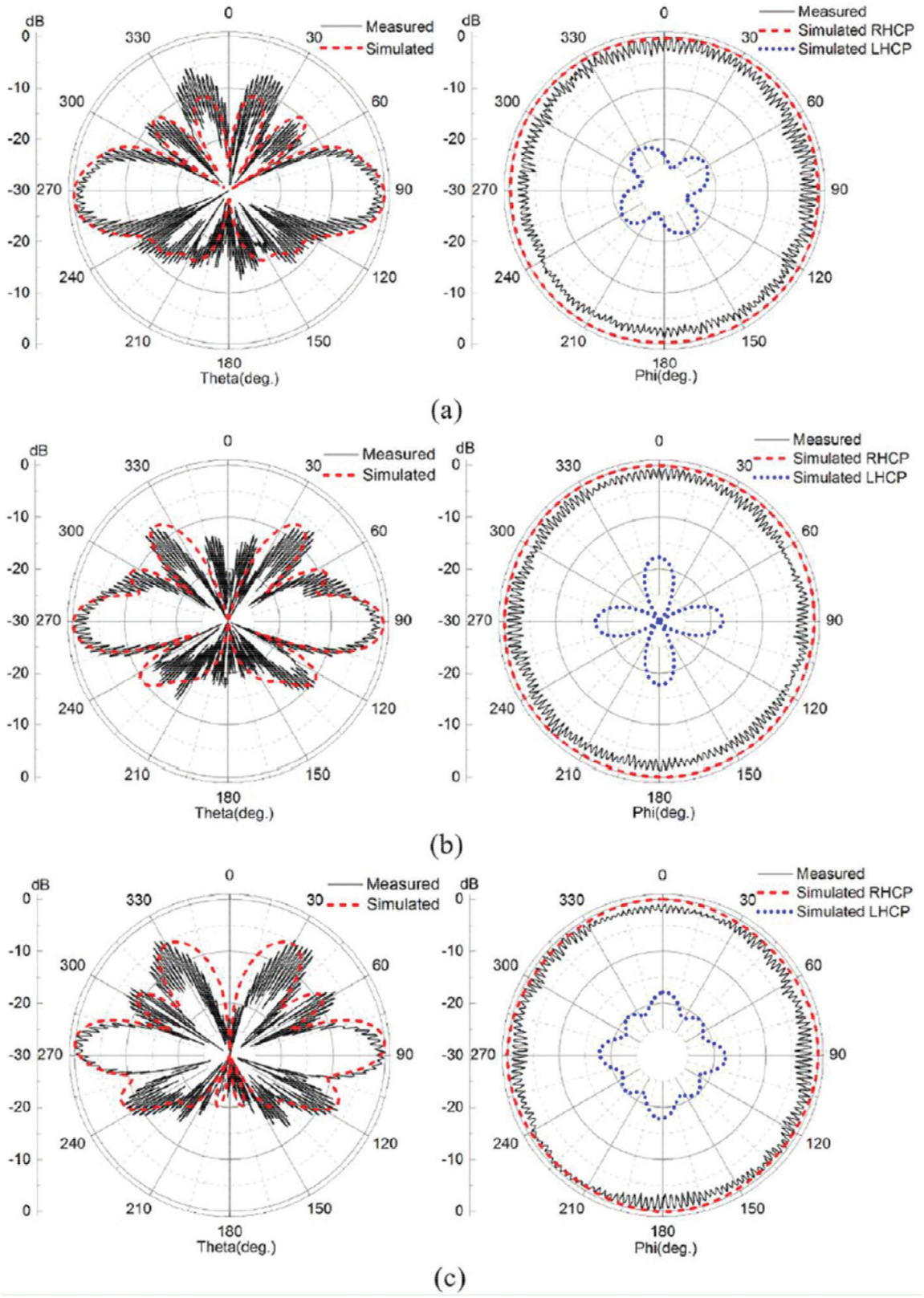

Figure 7. Simulated RHCP and LHCP normalized radiation patterns and measured normalized radiation pattern in the E-plane (*yz*-plane on the left) and the omnidirectional plane (*xy*-plane on the right). (a) 5.2 GHz. (b) 5.5 GHz. (c) 5.8 GHz.

3. Dual circularly polarized omnidirectional antenna with slot array on coaxial cylinder

Further, we introduce the dual circularly polarized omnidirectional antenna which has two ports in its two sides to realize dual circularly polarized property. The two ports are assigned in its two sides as left hand circularly polarized (LHCP) port and right hand circularly polarized (RHCP) port, respectively. The proposed antenna achieves a bandwidth of 16.4% ranging from 5.05 to 5.95 GHz with an isolation higher than 15 dB between the two CP ports, and the return loss (RL) is lower than -10 dB within the bandwidth in both of the two ports. From the measured results, the average axial ratio (AR) of the proposed antenna in omnidirectional plane is lower than 1.5 dB.

3.1. Antenna structure

As shown in **Figure 8**, the proposed dual omnidirectional CP antenna is based on the single CP omnidirectional antenna represented in literature [17] constructed with coaxial cylinder structure. Two ports are assigned in the two sides of the coaxial cylinder as left hand circularly polarized (LHCP) port and right hand circularly polarized (RHCP) port, respectively. The characteristic impedance of the coaxial cylinder is designed as 50 Ω in this section, which is the same as the characteristic impedance of the two SMA adaptor ports. The coaxial tapered line is in both of the two sides between the slot arrays and the two SMA adaptor ports, and it achieves the goal of port match.

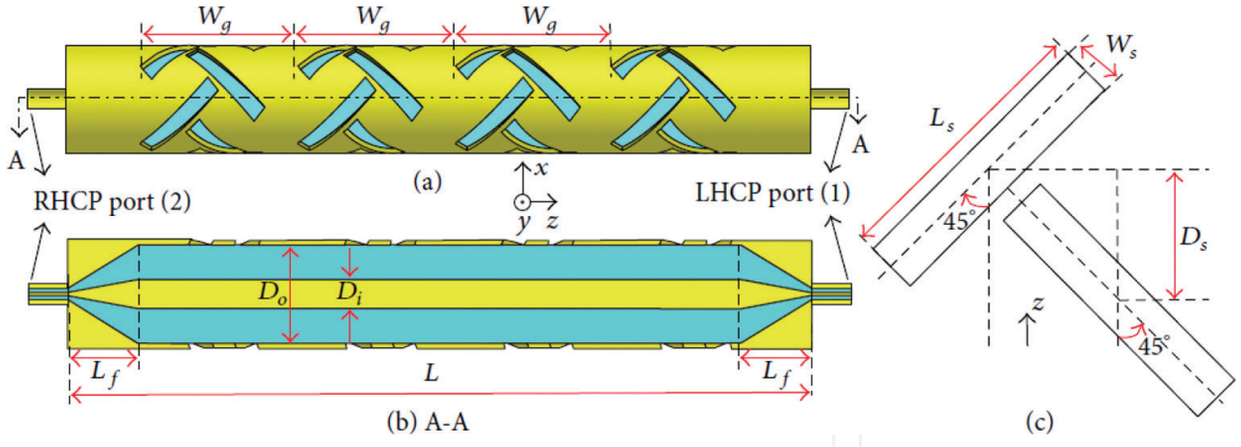

Figure 8. Geometry of the omnidirectional dual circularly polarized (CP) antenna. (a) Side view. (b) A-A section view. (c) Geometry of the slot pairs.

The basic radiation elements are slots in the out conductor of the coaxial cylinder. There are four circles of slots along the axis of the coaxial cylinder. Each circle of the slots includes 8 slots which are perpendicular to each other and symmetrically arranged around the coaxial cylinder axis in the out conductor. Every circle of the slots can be seen as four perpendicular slot pairs around the axis.

http://dx.doi.org/10.5772/66011

The structure of the perpendicular slot pairs is shown in **Figure 9**. Each of the slots leans at an angle of 45° with the axis of the coaxial cylinder and the interval of the two perpendicular slots is $\lambda g/4$ (λg is the medium wavelength) along the feed direction. In that case, the electric fields radiated from the slot pairs are vertical with each other and have a 90° phase difference, so the circularly polarized wave is generated. For the distance of the $\lambda g/4$ between the adjacent pairs of slots, the reflection power from radiation slots back to the feeding point is cancelled. As a slot antenna, the slot in the out conductor of the coaxial cylinder can be equivalent as magnetic dipole with a length of $\lambda g/2$ in the vertical direction with the axis. Four of the slot pairs symmetrically surrounding the coaxial cylinder axis achieve the omnidirectional coverage character. Four circles of the slot pairs, which are identical with each other, are arranged along the axis to constitute the slot array which will provide a higher gain. To achieve the omnidirectional pattern, the electromagnetic wave radiated from every circle of slots should be of the same phases, so the four circles of the slot are arranged with a distance of λg.

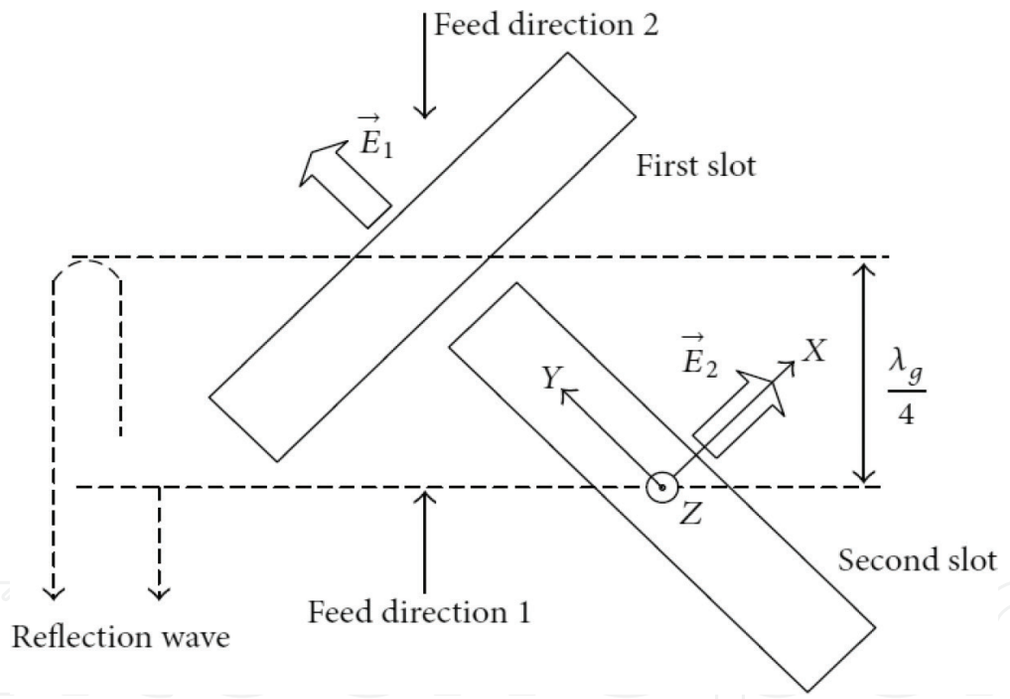

Figure 9. The adjacent perpendicular slot pairs.

It is a symmetrical structure antenna. The thickness of the out conductor of the coaxial cylinder is t = 1.3 mm, and the space between the out conductor and the inner conductor of the coaxial cylinder is filled with Teflon medium with a permittivity of ε_r = 2.1. The proposed antenna is simulated and optimized by CST and the optimized geometric parameters are summarized in **Table 2**.

L	153.5 mm	Wg	40 mm
D_i	7.6 mm	Do	28 mm
L_s	24.4 mm	Ws	4.3 mm
D_s	11.8 mm	Lf	18 mm

Table 2. Optimized geometric parameters of the omnidirectional CP antenna.

3.2. Design principle

Figure 9 shows two adjacent slots from all the slots in the out conductor, which are perpendicular to each other. The reference coordinate system is created with the slot pairs, whose y- and x-axes are of the same direction with the polarization of the electric fields radiated by the two slots, respectively, and the +z-axis is the same direction with the propagation direction of the electric fields [10, 18]. It is assumed that the total electric fields are $\vec{E}$ and the fields radiated from the first slot and the second slot are $\vec{E}_1$ and $\vec{E}_2$, respectively. Then their relation is

$$\vec{E} = \vec{E}_1 + \vec{E}_2 = E_x\vec{a}_x + E_y\vec{a}_y \tag{1}$$

For the distance of the two slots, it is supposed that the amplitude of the E_x and E_y is E_{x0} and E_{y0} ($E_{x0} > 0$, $E_{y0} > 0$), and compared to E_x, E_y is laggard in phase with a difference of ϕ. Then Eq. (1) can be changed as

$$\vec{E}(z, t) = E_{x0}\cos(wt - kz)\vec{a}_x + E_{y0}\cos(wt - kz - \phi)\vec{a}_y \tag{2}$$

where

$$\begin{aligned} E_x(z, t) &= E_{x0}\cos(wt - kz)\vec{a}_x \\ E_y(z, t) &= E_{y0}\cos(wt - kz - \phi)\vec{a}_y \end{aligned} \tag{3}$$

The relation between $E_x(z, t)$ and $E_y(z, t)$ can be concluded from Eq. (3):

$$\left[\frac{E_x(z, t)}{E_{x0}}\right]^2 + \left[\frac{E_y(z, t)}{E_{y0}}\right]^2 - \frac{2E_x(z, t)E_y(z, t)}{E_{x0}E_{y0}}cos\phi = \sin^2\phi \tag{4}$$

Since the distance of the two slots in the feed direction is $\lambda_g/4$, the phase difference is $\phi = \pm 90°$. It is supposed that the amplitude of electric fields is $E_{x0} = E_{y0} = E_0$, then from Eq. (4):

$$E_x^2(z, t) + E_y^2(z, t) = E_0^2 \tag{5}$$

It can be seen from Eq. (3) that the amplitude of $\vec{E}(z, t)$ will not change with time t, and the angles between the polarization direction of $\vec{E}(z, t)$ and +x-axis direction are

$$\alpha = \tan^{-1}\frac{E_0\cos\left(wt - kz \pm \frac{\pi}{2}\right)}{E_0\cos(wt - kz)} = \tan^{-1}[\pm\tan(wt - kz)] = \mp(wt - kz) \tag{6}$$

In any positions, z is a constant, and the polarized vector direction of the field $\vec{E}(z, t)$ is rotary with a constant angular frequency ω by the increasing of t. As shown in **Figure 11**, when excited as fed direction 1, the phase of E_y is laggard compared to the phase of E_x, so $\phi = 90°$ and $\alpha = \omega t$. The electric fields vector direction is anticlockwise, so it is right hand circularly polarized (RHCP) wave. When excited as fed direction 2, the phase of E_y exceeds the phase of E_x, so $\phi = -90°$ and $\alpha = -\omega t$. The electric fields vector direction is clockwise, so it is left hand circularly polarized (LHCP) wave. Comparing **Figure 11** with the slots distribution in **Figure 11**, the RHCP port and LHCP port are corresponding with fed direction 1 and fed direction 2, respectively.

For the different distances of the two slots relative to the fed port, the electric fields amplitude of the two slots is unequal $\left(E_{x0} \neq E_{y0}\right)$. This is an influence factor of the axial ratio and their relation is reflected by the axial ratio character of the antenna.

3.3. Results and discussion

Simulated and measured results of the proposed antenna are presented in this section. To measure the LHCP property and RHCP property of the antenna, there are two steps. When port 1 (LHCP port) is excited and port 2 (RHCP port) is terminated with a 50 Ω load, the antenna generates the LHCP radiation and we get LHCP results, whereas when port 2 is excited and port 1 is terminated with a 50 Ω load, the antenna generates the RHCP radiation and we get RHCP measurement results. **Figure 10** shows the antenna structure and the test scenario of the omnidirectional dual CP antenna.

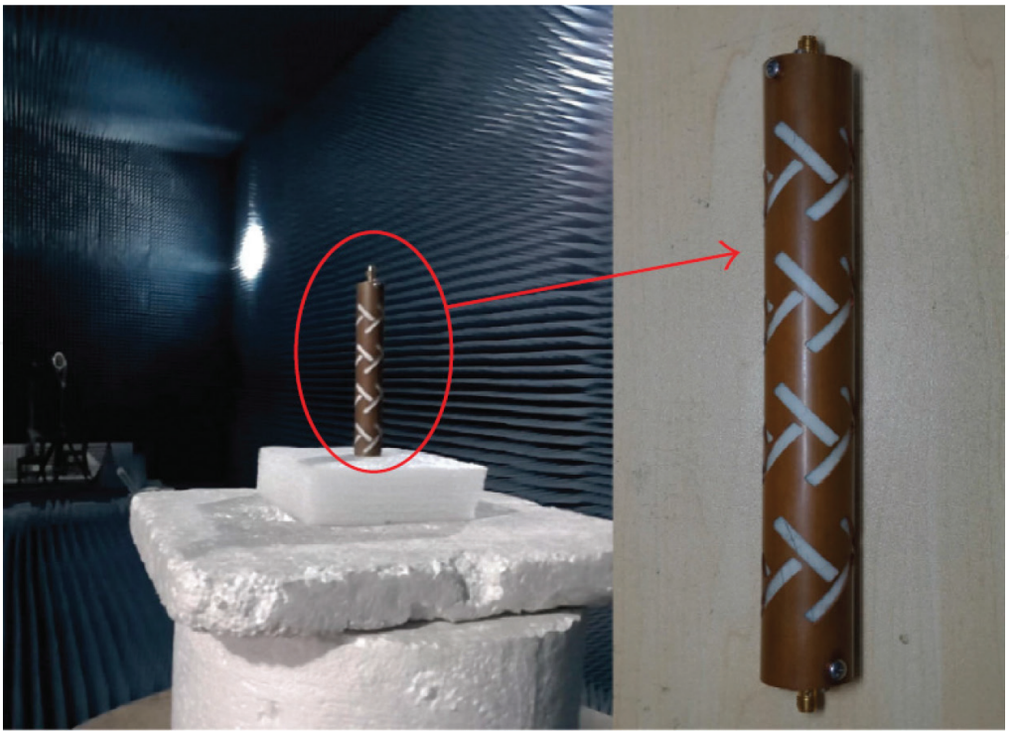

Figure 10. Photograph of the omnidirectional dual CP antenna being tested in the anechoic chamber.

The measured *S*-parameters results are shown in **Figure 11**. The proposed antenna achieves a bandwidth of 16.4% at 5.05–5.95 GHz, during which the bandwidth isolation between the two ports is higher than 15 dB, and both of the measured |*S*11| and |*S*22| values are lower than -10 dB. The reflection of the two ports is small and the isolation between the two ports is high, which reflects that the antenna works well with two polarizations.

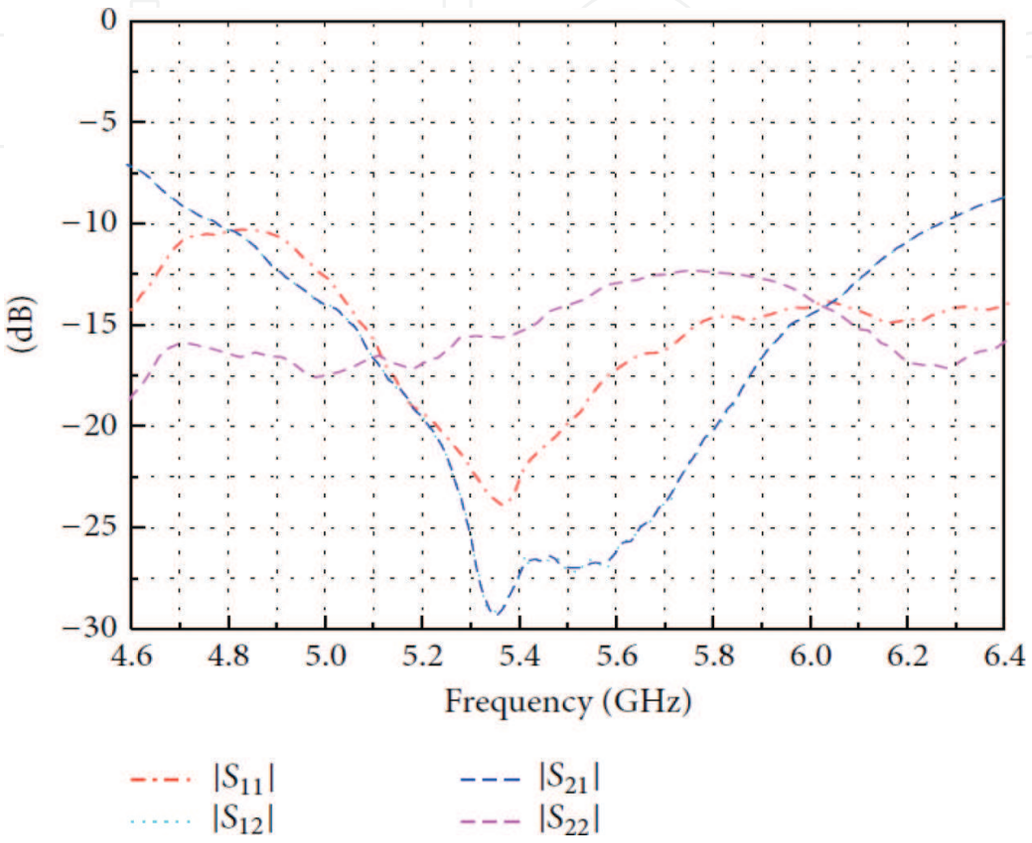

Figure 11. Measured *S*-parameters results.

Figure 12 shows the simulated and measured normalized copolarization and cross-polarization radiation patterns when excited RHCP port and LHCP port, respectively, are in the *xy*-plane (omnidirectional plane) and *xz*-plane at 5.1, 5.5, and 5.9 GHz. From the measured radiation pattern results of the *xy*-plane, the proposed antenna performs a good omnidirectional character.

It is noted that the measured radiation patterns have the same trend with the simulated radiation patterns, but there are still a few discrepancies between measured results and simulated results. The reasons for this difference are mainly because of the machine error and the imprecision of the medium. It can be also seen from cross-polarization results that the cross-polarization is more than 15 dB lower than the copolarization in both *xy*-plane and *xz*-plane. The measured axial ratio patterns that only excited LHCP port in *xy*-plane and *xz*-plane at 5.1, 5.5, and 5.9 GHz are shown in **Figure 13**. It can be seen that the axial ratio is below 3 dB in the omnidirectional plane within the operation bandwidth. Comparing the radiation patterns and

http://dx.doi.org/10.5772/66011

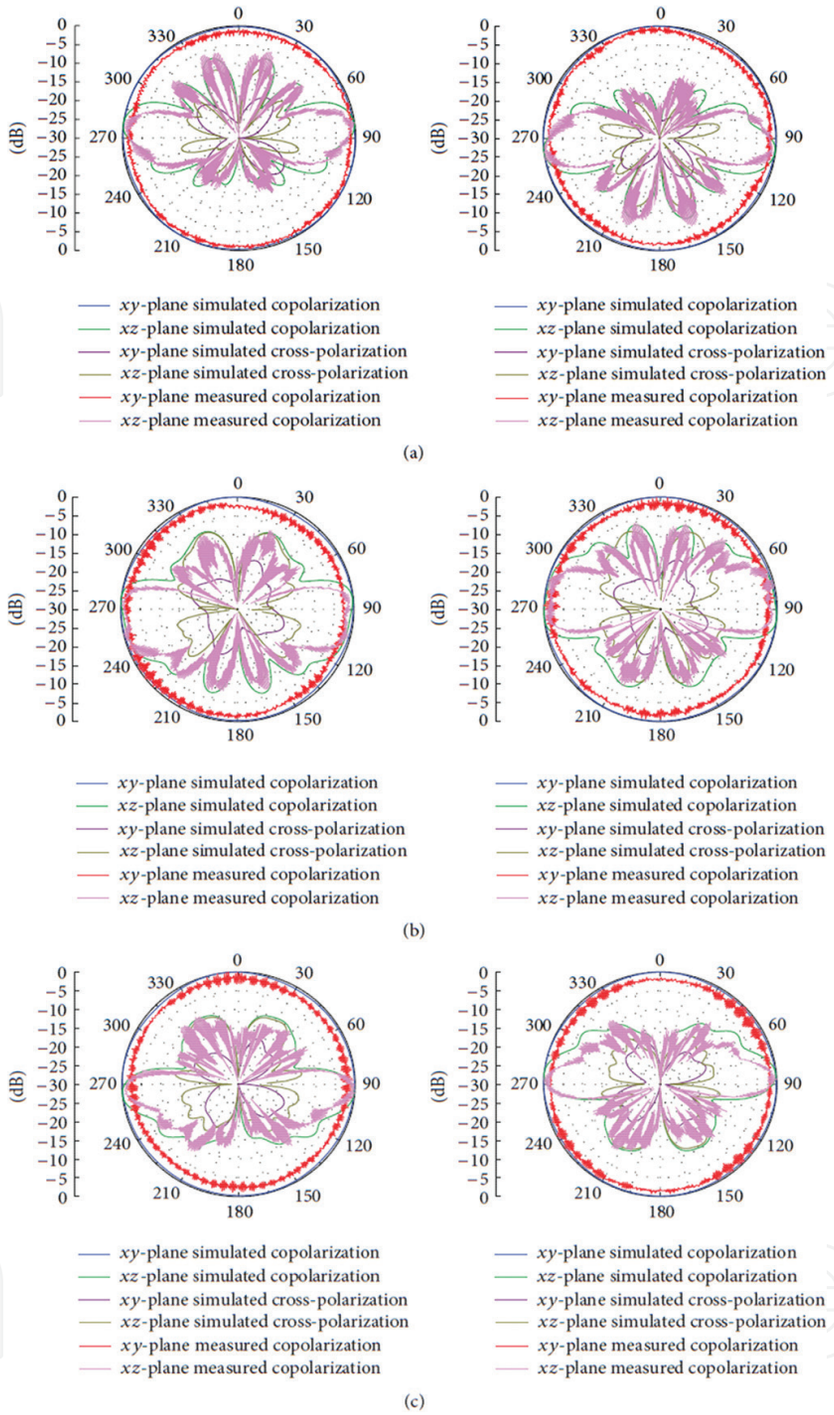

Figure 12. Simulated and measured LHCP (in left) and RHCP (in right) normalized copolarization and cross-polarization radiation patterns in the *xy*-plane (omnidirectional plane) and *xz*-plane. (a) 5.1 GHz, (b) 5.5 GHz, and (c) 5.9 GHz.

axial ratio patterns results, the axial ratio is lower than 3 dB during the half power beam width. When only excited the RHCP port, the axial ratio is below 3 dB in the omnidirectional plane which is similar as show **Figure 13**. It can be noted that the axial ratio patterns in the *xy*-plane are small ripples. From the generation principle of the dual CP wave as analyzed in Section

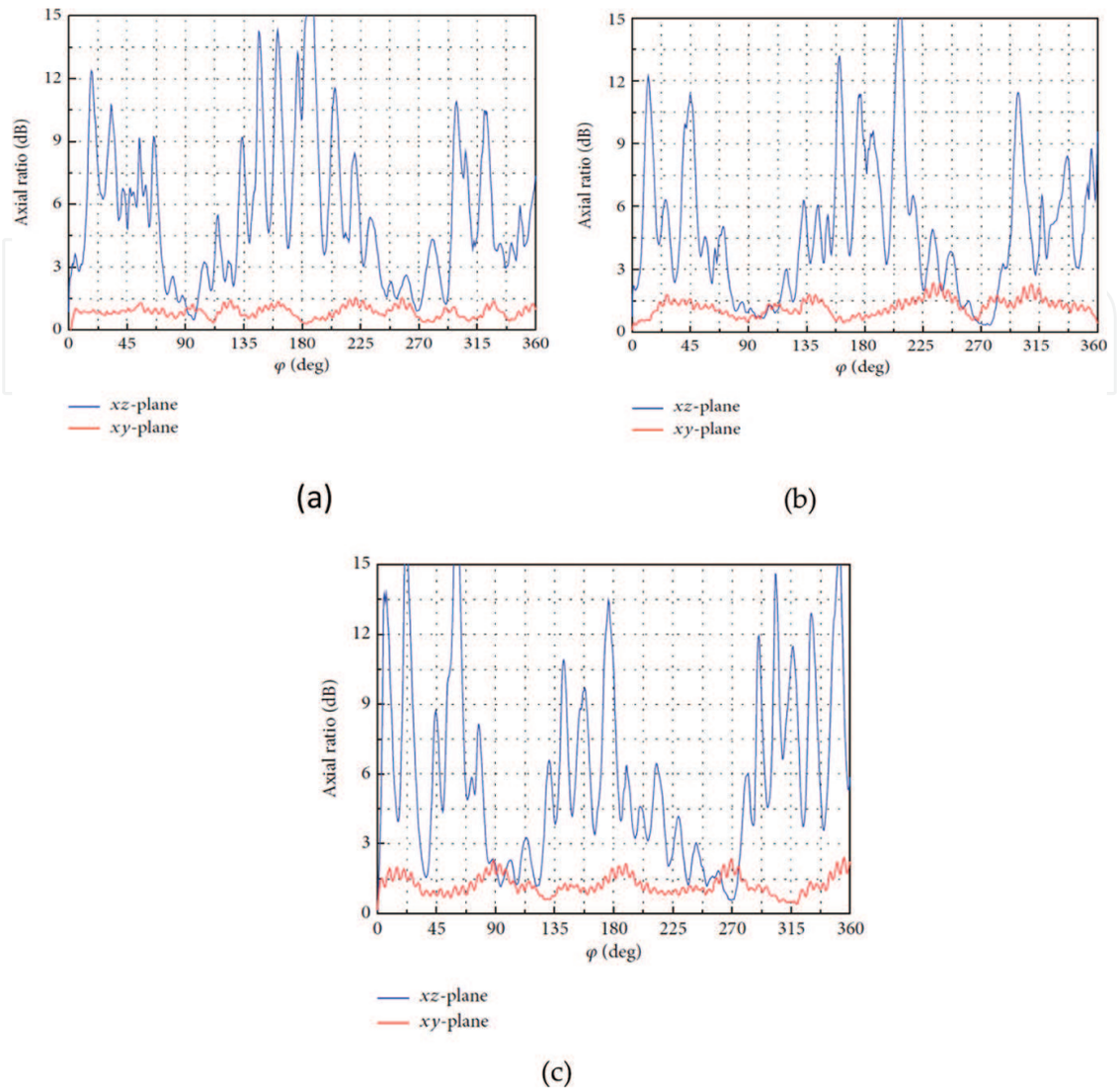

Figure 13. Measured axial ratio patterns in *xy*-plane and *xz*-plane. (a) 5.1 GHz, (b) 5.5 GHz, and (c) 5.9 GHz.

2.2, the axial ratio in the vertical direction with the slot pairs will be the best and the value will be the minimum, while in the other nonvertical direction with the slot pairs the axial ratio will deteriorate. Because four slot pairs are arranged around the axis of coaxial cylinder in the out conductor, the slot pairs are noncoplanar. When rotated around the axis of the antenna, the axial ratio pattern in the *xy*-plane will be small rippled almost regularly as the symmetrical antenna structure in different ϕ directions.

The measured gain and average axial ratio in the omnidirectional plane results are shown in **Figure 14**. It can be seen that the gain is from 4 to 6 dBic within 5.0–6.0 GHz, and the average axial ratio in *xy*-plane is below 1.5 dB within the bandwidth. **Figure 15** shows the simulated total efficiency of the proposed antenna. It can be noted from the efficiency results that the total efficiency of the antenna from 5.1 to 5.9 GHz is from 86.9 to 93.5%, so the antenna works with very high efficiency within its operation bandwidth.

http://dx.doi.org/10.5772/66011

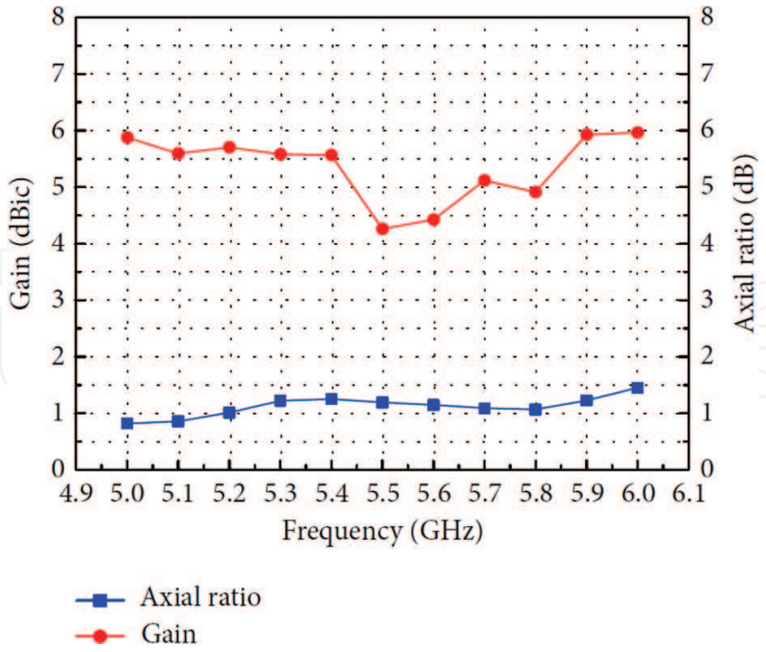

Figure 14. Measured gain and average axial ratio in the omnidirectional plane.

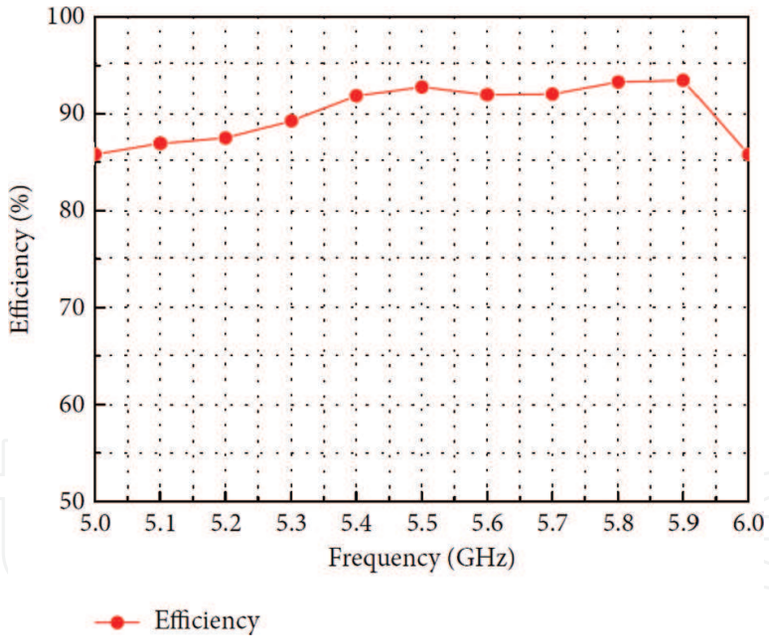

Figure 15. The total efficiency results of the proposed antenna.

4. Compare with others

Here, we compare the proposed omnidirectional CP antenna with others' work in **Table 3**. Our proposed antenna impedance bandwidth, the CP bandwidth is the widest and the gain is largest, although it is the longest.

5. Conclusion

Antenna type	Ref.	Size	Band width	3 dB AR band width	Gain
Omnidirectional CP antenna	[19]	3.175 × 56 × 56 mm^3	0.539% (1.481–1.489 GHz)	AR = 2.03 dB (1.481–1.489 GHz)	LHCP: -0.73 to -0.14 dBi RHCP: -21.02 to -17.66 dBi
Dual band omnidirectional CP antenna	[2]	3.175 × 33 × 33 mm^3	0.5% (low freq) 1.1% (high freq)	1.57 dB/low freq 0.86 dB/high freq	Low freq: -0.59 to 1 dBi High freq: -0.94 to -0.2 dBi
Omnidirectional CP antenna	[8]	$0.22\lambda_0 \times 0.22\lambda_0 \times 0.07\lambda_0$	3.56%	3.56%	1.5 dBi
Omnidirectional CP antenna	[7, 20]	15 × 90 × 90 mm^3	14%	RHCP: 1.35–1.6 GHz LHCP: 1.35–1.65 GHz	RHCP: 0.8 dBi LHCP: 0.1 dBi
DRA omnidirectional CP antenna	[5, 6]	Small	7%	12.3% (2.21–2.5 GHz)	<2 dBi
omnidirectional dual CP antenna	Proposed	190 × 30 × 30 mm^3	16.4% (5.05–5.95 GHz)	14.5% (5.1–5.9 GHz)	7 dBi

Table 3. Compare the proposed antenna with others' research results.

The omnidirectional CP antenna with slot array on coaxial cylinder with stable high gain in a wide bandwidth was studied, and the results between measurement and simulation are almost congruent. The improved omnidirectional dual CP antenna is presented too, which achieves the omnidirectional dual CP property by arranging perpendicular slot pairs around and along the coaxial cylinder axis in the out conductor. These antennas have perfectly symmetric structure, so they are easy to change the working frequency band by changing the size of the antenna. For the omnidirectional coverage property and dual CP property, the antennas are valuable in the RF receiver.

Acknowledgements

This work was supported by the National Natural Science Foundation under Grants 61471240,61571289, and 61571298 and the Project of "SMC Excellent Young Faculty."

Author details

Bin Zhou, Junping Geng*, Xianling Liang, Ronghong Jin and Guanshen Chenhu

*Address all correspondence to: gengjunp@sjtu.edu.cn

Department of Electric Engineering, Shanghai Jiao Tong University, Shanghai, China

http://dx.doi.org/10.5772/66011

References

[1] K. Sakaguchi and N. Hasebe, "A circularly polarized omnidirectional antenna," in Proc. 8th ICAP, 1993, pp. 477–480.

[2] B. C. Park and J. H. Lee, "Dual-band omnidirectional circularly polarized antenna using zeroth- and first-order modes," IEEE Antennas Wireless Propag. Lett., vol. 11, pp. 407–410, 2012.

[3] A. Narbudowicz, X. L. Bao, and M. J. Ammann, "Dual-band omnidirectional circularly polarized antenna," IEEE Trans. Antennas Propag., vol. 61, no. 1, pp. 77–83, 2013.

[4] W. Q. Cao, A. J. Liu, and B. N. Zhang, "Dual-band spiral patch-slot antenna with omnidirectional CP and unidirectional CP properties," IEEE Trans. Antennas Propag., vol. 61, no. 4, pp. 2286–2289, 2013.

[5] Y. M. Pan, K. W. Leung, and K. Lu, "Omnidirectional linearly and circularly polarized rectangular dielectric resonator antennas," IEEE Trans. Antennas Propag., vol. 60, no. 2, pp. 751–759, 2012.

[6] W. W. Li and K. W. Leung, "Omnidirectional circularly polarized dielectric resonator antenna with top-loaded alford loop for pattern diversity design," IEEE Trans. Antennas Propag., vol. 61, no. 8, pp. 4246–4256, 2013.

[7] B. Li, S. Liao, and Q. Xue, "Omnidirectional circularly polarized antenna combining monopole and loop radiators," IEEE Antennas Wireless Propag. Lett., vol. 12, pp. 607–610, 2013.

[8] Y. Yu, Z. Shen, and S. He, "Compact omnidirectional antenna of circular polarization," IEEE Antennas Wireless Propag. Lett., vol. 11, pp. 1466–1469, 2012.

[9] X. Quan, R. Li, and M. M. Tentzeris, "A broadband omnidirectional circularly polarized antenna," IEEE Trans. Antennas Propag., vol. 61, no. 5, pp. 2363–2370, 2013.

[10] K. Iigusa, T. Teshirogi, M. Fujita, S.-I. Yamamoto, and T. Ikegami, "A slot-array antenna on a coaxial cylinder with a circularly polarized conical beam," Electron. Commun. Jpn. Pt. I, vol. 83, pp. 74–87, 2000.

[11] W. Croswell and C. Cockrell, "An omnidirectional microwave antenna for use on spacecraft," IEEE Trans. Antennas Propag., vol. 17, no. 4, pp. 459–466, 1969.

[12] C. Y. Yu, T. H. Xu, and C. J. Liu, "Design of a novel UWB omnidirectional antenna using particle swarm optimization," Intl. J. Antennas Propag., vol. 2015, Article ID 303195, 7 p., 2015.

[13] M. Khalily, M. R. Kamarudin, M. Mokayef, and M.H. Jamaluddin, "Omnidirectional circularly polarized dielectric resonator antenna for 5.2-GHz WLAN applications," IEEE Antennas Wireless Propag. Lett., vol. 13, pp. 443–446, 2014.

[14] X. D. Bai, X. L. Liang, M. Z. Li, B. Zhou, J. Geng, and R. Jin, "Dual-circularly polarized conical-beam microstrip antenna," IEEE Antennas Wireless Propag. Lett., vol. 14, pp. 482–485, 2015.

[15] D. Yu, S.-X.Gong, Y.-T.Wan, and W.-F.Chen, "Omnidirectional dual-band dual circularly polarized microstrip antenna Using TM01 and TM02 modes," IEEE Antennas Wireless Propag. Lett., vol. 13, pp. 1104–1107, 2014.

[16] X.-L. Quan and R.-L. Li, "Broadband dual-polarized omnidirectional antennas," in Proceedings of the IEEE Antennas and Propagation Society International Symposium (APSURSI '12), pp. 1–2, IEEE, Chicago, Ill, USA, July 2012.

[17] B. Zhou, J. P.Geng, X. D. Bai, L. Duan,X. Liang, and R. Jin, "An omnidirectional circularly polarized slot array antenna with high gain in a wide bandwidth," IEEE Antennas Wireless Propag. Lett., vol. 14, pp. 666–669, 2015.

[18] M. E. Bialkowski and P. W. Davis, "Linearly polarized radialline slot-array antenna with a broadened beam," Microwave Optical Technol. Lett., vol. 27, no. 2, pp. 98–101, 2000.

[19] B.C. Park and J.H. Lee, "Omnidirectional circularly polarized antenna utilizing zeroth-order resonance of epsilon negative transmission line," IEEE Trans. Antennas Propag. vol. 59, no. 7, pp. 2717–2721, 2011.

[20] B. Li and Q. Xue, "Polarization-reconfigurable omnidirectional antenna combining dipole and loop radiators," IEEE Antennas Wireless Propag. Lett., vol. 12, pp. 1102–1105, 2013.